
Global Toxicology 2020: Titanium dioxide food grade induces reactive oxygen species production and cell cycle arrest in colorectal cancer cells- Carolina Rodríguez-Ibarra, GROW Institute of Oncology and Developmental Biology, Mexico

Abstract

E171 is known as Titanium dioxide food grade, is an additive commonly used as a whitening agent in food and as excipient in toothpaste and pharmaceuticals at quantum satis in the European Union, meaning there is no specific quantity restriction. Although E171 has been considered safe, inhalation of industrial titanium dioxide has been classified as a possible carcinogen, which has raised concerns about possible adverse outcomes when ingested. Oral E171 administration exacerbates tumour formation in murine models of colorectal cancer. However, cellular mechanisms related to carcinogenesis have not been fully investigated. The aim of this work was to investigate cellular mechanisms of toxicity induced by an acute E171 exposure in colon epithelial cells and also analyze if those alterations are permanent or can be reversed. Acute E171 exposure induced an increase in cell granularity and reactive oxygen species generation, which were not accumulative but were lasting for at least 2 days, however alterations in cell cycle distribution observed during the acute exposure were reverted after 2 days. Finally, no internalization of particles in the nuclei was detected but only perinuclear localization.

Introduction

Since 1969, the European Union affirmed the utilization of food-grade titanium dioxide (TiO₂) known as E171 shading food added substance. TiO₂ is a white shade utilized as a shading operator in many goods, for example, food and individual consideration items (1–4). E171 is utilized in food, for example, in serving of mixed greens dressing, gum, icing, treats and confections (5) and despite the fact that TiO₂ is sourced from rutile, anatase and brookite, the European Union permits E171 in the food just as anatase structure (5). As indicated by the European Union, E171 has a place with the Group II: food hues approved at quantum satis which signifies 'no maximum limit level is determined and that it ought to be utilized at levels not higher than considered important for the item' (5). In the USA, the Food and Drug Administration permits the food added substance E171 as long as it doesn't surpass 1% by complete load of the item (6).

Inward breath concentrates with TiO₂ presentation have shown unfavorable impacts, including 8-OHdG DNA adduct arrangement and genotoxicity (7–11). In 2010, the International Agency for Research in Cancer characterized TiO₂ as conceivable cancer-causing agent to people (Group 2B) (12). Consequently, worry about oral utilization of E171 has been raised (13–17).

E171 is a blend of smaller scale estimated particles (MPs; 64%) and nano-sized particles (NPs; 36%) (4) and the NPs extent is required to increment in the decades to come (18). NPs have a higher surface region than MPs permitting them to have more communication with the cells, which thus can prompt reactive oxygen species (ROS) arrangement after disguise. The presentation of cells to particles can prompt oxidative worry as has been appeared for different particles (19,20). Cell oxidative pressure

initiated by presentation to TiO₂ NPs could prompt potential non-specific DNA harm through the age of the superoxide anion (21), the antecedent of the profoundly responsive hydroxyl radical, which is a notable strong mutagen that assaults DNA (22–24). MPs of TiO₂ can amass in lymphoid tissue after oral ingestion (25) and furthermore in macrophages of human gut-related lymphoid tissue (26). The nano-sized division can cause pallor and genotoxicity by intragastric organization in a rodent test model (27). Also, we recently found that intragastric E171 organization improved the tumor development, actuated artificially by azoxymethane/dextran sodium sulfate (AOM/DSS) in colon of uncovered mice (28). The cell instrument of harm after internalization of E171, MPs and NPs has not been set up yet, however ROS arrangement could add to the acceptance of cell harm. In this manner, we estimate that nano-sized and small scale measured parts of E171 could have an alternate commitment in ROS arrangement and enlistment of DNA harm. To test our theory, we estimated ROS formation incited by E171, TiO₂ MPs and NPs in sans cell conditions utilizing electron spin reverberation (ESR)/paramagnetic reverberation spectroscopy perceived as a 'highest quality level' and best in class apparatus for recognition and measurement of ROS and free radicals (29,30). This method is especially favored in considering the impact of E171 as photocatalytic properties of TiO₂ cause obstruction in fluorescent or chemiluminescence measures (31,32). Moreover, we decided the DNA harm actuated by these various kinds of particles by the comet and small scale cores recurrence (MN) measures in colon-determined cell lines presented to non-cytotoxic E171, TiO₂ MPs and NPs fixations.

Materials and techniques

TiO₂ particles properties

E171 was mercifully given by the Sensient Technologies Company in Mexico. TiO₂ MPs were generally made by PlasmaChem with a normal size of 535 nm described by transmission electron microscopy. TiO₂ NPs were bought at Io-Li-Tec (Germany) and are 99.5% anatase with molecule size of 10–25 nm and a particular surface region of 50–150 m²/g as indicated by maker's data. All particles were sanitized at 121°C for 20 min earlier use.

Scattering of TiO₂ particles

TiO₂ particles (E171, NPs or MPs) were weighed into glass tubes and scattered in 0.05% cow-like serum egg whites (BSA) Dulbecco's altered Eagle's medium (DMEM) (Sigma Aldrich), Hank's balanced salt arrangement (HBSS) enhanced with Mg²⁺ and Ca²⁺ (Life Technologies, The Netherlands) or phosphate-supported saline at a convergence of 1 mg/mL. Particles stock suspensions were sonicated in a shower sonicator (Branson 2200, 40 kHz) for 30 min and further used to set up the weakenings required for presentation.

For the MN measure, 1 mg of E171 particles was scattered in medium with 10% fetal ox-like serum (FBS), in light of the fact that 10% FBS is prescribed for MN tests so as to keep away from bogus positive outcomes in cell societies (33).

Portrayal of TiO₂ particles with electron microscopy and DLS

Scios DualBeam FIB/(SEM, 20 kV, Holland) was utilized at vary ent amplification from ×50 000 for the MPs to ×150 000 for E171 and NPs to assess the size and morphology of E171, MPs and NPs. All examples were spread on carbon tape and falter covered with gold before examining electron minuscule (SEM) investigation. The size of the particles were estimated on a few pictures by the product Image J, in excess of 100 particles were estimated for each example.

To describe the hydrodynamic size conveyance and the zeta capability of the TiO₂ particles (E171, NPs and MPs), a Malvern Nano ZS (Malvern Instruments, UK) dynamic light dissipating (DLS)

instrument furnished with a 633 nm helium–neon laser was utilized. Two agent scatterings 0.001 and 1 mg/mL (compare ing to 0.143 and 143 $\mu\text{g}/\text{cm}^2$, separately) scattered in 0.05% BSA DMEM or HBSS enhanced with Mg^{2+} and Ca^{2+} or McCoy +10% FBS were set up in copy and moved in an expendable collapsed hairlike (DTS 1060, Malvern Instruments). Estimations were acted in triplicate at 25°C, with equilibration time set at 0 s, a thickness at 0.8872 cP and a refracting list of 1.330. The zeta potential shows the possible steadiness of the colloidal framework which in our investigation is strong particles scattered in fluid (0.05% BSA medium, 10% FBS medium or support). At the point when the zeta expected have huge negative or positive potential (± 30 mV), they will in general repulse each other where there is no inclination to agglomerate. Interestingly, if the particles have low zeta likely qualities, there is no power to pre-vent the particles appending to one another and agglomerating.

Cell culture of colon Caco-2 cells

The human colon carcinoma cell line Caco-2 was gotten from the American Type Culture Collection (ATCC® HTB-37™) and refined in DMEM enhanced with glutamine, glucose, sodium pyruvate, penicillin/streptomycin and 10% warmth inactivated FBS. Cells were developed and kept up at 37°C in a humidified hatchery containing 5% carbon dioxide (CO_2). For tests, Caco-2 cells were seeded in 21 cm^2 culture dishes and developed for 3 days to arrive at 80–100% confluency in 10% FBS medium so as to get ± 3.106 cells/dish.

Cell culture of colon HCT116 cells

Because of the heterogeneity and hereditary shakiness of the Caco-2 cells, we utilized the suggested HCT116 cell line for MN measures, which has genomic dependability (34). The human colon adenocarcinoma (HCT116) cell line was acquired from the American Type Culture Collection (ATCC® CCL-247™). HCT116 cells were brooded in a 37°C and 5% CO_2 environment and kept up in McCoy 5a-mod-ified medium with 1.5 mM l-glutamine and 2.2 mg/mL sodium bicarbonate (in vitro, no. feline. ME-042) enhanced with 10% FBS (Biowest, no. feline. US1520).

Cytotoxicity of TiO_2 particles to Caco-2 cells

Before presentation, colon Caco-2 cells were refined for 3 days in 10% FBS medium and from there on washed twice with HBSS. Then, cells were presented to a scope of fixations E171, MPs or NPs (0.143–143 $\mu\text{g}/\text{cm}^2$ which counterparts to 0.001–1 mg/mL), scattered in 0.05% BSA medium, for 24 h. Three distinctive feasibility/cytotox-icity tests were performed: lactate dehydrogenase (LDH), thiazolyl blue tetrazolium bromide (MTT) and Trypan blue examines, two of them indicated association between the test and the particles. At that point, the reasonability of the cells was surveyed with Trypan blue test. After 24 h, cells were washed twice with HBSS followed by trypsinization of the cells and checked with a programmed cell counter (Logos Biosystems) where Trypan blue stain (0.4%) was added to the cell suspension (1:1). Non-cytotoxic centralizations of E171, TiO_2 NPs or MPs were chosen dependent on feasibility ($>80\%$) of the cells. Triton-X-100 (Sigma-Aldrich) (1%) was added to the cells as positive control.

Cytotoxicity of E171 to HCT116 cells

For HCT116 cells, the practicality was evaluated by Trypan blue test. After 24 h of introduction to 0, 5, 10, 50 and 100 $\mu\text{g}/\text{cm}^2$ (0, 50, 100, 500 and 1000 $\mu\text{g}/\text{mL}$, separately) of E171, cells were washed twice with HBSS followed by trypsinization and cells were checked with a Neubauer chamber. Living cells were recognized by including Trypan blue stain (0.4%) to 10 μL of cell suspension (1:2).

ROS development evaluated by ESR spectroscopy

ROS evaluation in acellular conditions

Particles were scattered and stock suspensions of 1 mg/mL were serially weakened in 0.05% BSA medium, HBSS enhanced with Ca²⁺ and Mg²⁺ or PBS (1×). To survey the limit of ROS arrangement by TiO₂ particles, suspensions were hatched in a CO₂ hatchery at 37°C with 50 mM 5,5-dimethyl-1-pyrroline N-oxide (DMPO) for 30 min. Hydrogen peroxide (H₂O₂; 1 mM) was added to particles suspensions to survey the responses that could occur in a salt situation. After brooding, homogenized particles suspension was taken up into a 100-μL glass slender. Radical development was estimated by ESR spectroscopy.

ROS evaluation in uncovered cell societies

The test was performed by the convention of Nymark et al. (35). To sum things up, Caco-2 cells (entry 24–32) were refined as clarified beforehand. Particles were scattered and stock suspensions of 1 mg/mL were sequentially weakened in scattering suspensions to get non-cytotoxic convergences of 0.143 and 1.43 μg/cm² (which equivalents to 0.001 and 0.01 mg/mL, individually). Earlier introduction, cells were washed twice with HBSS enhanced with Ca²⁺ and Mg²⁺. Cells were presented to non-cytotoxic groupings of E171, NPs or MPs in a CO₂ hatchery at 37°C for a few presentation times (30 min, 1, 2, 4, 6 and 24 h, individually). The most extreme sign was seen at 1 h presentation. Furthermore, H₂O₂ was included at a non-cytotoxic focus (20 μM, as indicated by cytotoxicity tests by Briedé et al. (36) to cells along with particles suspensions to mirror an incendiary domain. Thirty minutes before closure the presentation, trap DMPO (50 mM) was added to the cells and brooded at 37°C. This hatching time was put together and tried for TiO₂ with respect to past time course analyzes performed by Hebels et al., where at 30 min the most elevated DMPO radical adduct focus was discovered (37). After introduction, cells were gathered by scratching and taken up into a 100-μL glass slim and radical arrangement was estimated by ESR spectrometry.

A similar convention was utilized for a co-presentation with AOM was included at a non-cytotoxic focus (20 μg/mL) to the cells along with particles suspensions. The focus AOM was affirmed as non-cytotoxic with Trypan blue practicality tests (information not appeared).

ESR spectroscopy estimations

Radical arrangement in light of non-cytotoxic centralizations of TiO₂ was estimated by ESR spectroscopy. Prior to utilize, DMPO was decontaminated by the convention of Hebels et al. (37). Stock solutions of DMPO were tried on forehand on •OH arrangement by H₂O₂ and ferrous sulfate (0.75 mM) to confirm the action of DMPO (information not appeared). In the wake of fixing, the narrow was quickly positioned in the resonator in the ESR spectrometer. All estimations were acted in obscurity. ESR spectra were recorded with indistinguishable conditions from Nymark et al. what's more, Hebels et al. (35,37).

DNA harm appraisal in Caco-2 cell societies by the comet measure

Cells were developed for 3 days to arrive at confluency of 80–90% and were washed twice with HBSS before introduction. Cells were presented to non-cytotoxic fixations E171, NPs or MPs in a CO₂ hatchery at 37°C for 24 h with or without 20 μg/mL AOM (Sigma Aldrich), a genotoxicant. Each condition was surveyed in copy. As a positive control, cells were uncovered for 30 min to 200 μM H₂O₂. The test was proceeded as portrayed by Hebels et al. (38). Comet show up analyses were investigated utilizing fluorescence magnifying instrument (Zeiss, Germany) at ×400 amplification utilizing submersion oil (beneficial Figure 2, accessible at Mutagenesis Online). A sum of arbitrarily chosen 50 cells were dissected per slide per analyze. Comet picture analysis program was utilized for measurement of DNA harm. Comet tail and force were estimated by utilizing Comet IV programming. The middle tail power was utilized as DNA harm pointer. All tests were made with four natural reproduces and in duplicate, each copy was put on two slides (n = 16).

Chromosome harm in HCT116 cells surveyed by MN measure

HCT116 cells were seeded 150 000 cells on 6 cm² coverslips. Cells were treated with 0, 5, 10, 50 and 100 µg/cm² (0, 50, 100, 500 and 1000 µg/mL individually) of E171 for 24 h. MN test can't be surveyed in cell societies presented to 100 µg/cm² or more since agglom-erates meddle with MN recognizable proof. MN examine was done as portrayed by Fenech (39). Quickly, to obstruct the cytokinesis and to get binucleated cells, after 24 h of treatment, the medium with E171 was evacuated and cells were washed with PBS and rewarded with 4.5 µg/mL of cytochalasin B (Cyt-B; Sigma-Aldrich, no. feline. C6762) for 24 h. After treatment with Cyt-B, the cells were fixed with 1 mL of paraformaldehyde 3% for 1 h and recolored with Hoescht 1:200 (Thermo Scientific, no. feline. 62249) at 37°C and steady fomentation for 1 h. The slides were scored utilizing an Axio Vert. A1 Carl Zeiss influenza orescence magnifying instrument at ×1000 amplification under oil inundation. To ascertain the recurrence of binucleated cells with MN and the fied as indicated by their number of micronucleus. The recurrence was communicated as the level of binucleated cells with micronucleus in 1000 binucleated cells. All analyses were made in triplicate.

E171 cooperation with kinetochore shafts

HCT116 cells were seeded (1.5×10^5 cells) on coverslips and a load of E171 particles were resuspended in cell culture medium flexible mented with FBS 10%. Cell societies were presented to last concentra-tions of 5, 10, 50 and 100 µg/cm² for 24 h. After presentation, cells were washed with PBS, fixed with 2% paraformaldehyde and permeabi-lised with an answer containing 0.1% sodium citrate and 0.1% Triton. Vague restricting locales were obstructed by hatching cells with 5% BSA, and afterward the cells were recolored with a 1:200 weakening of mouse monoclonal enemy of α -tubulin counter acting agent and 4',6-diamidino-2-phenylin-give (1 µg/mL), trailed by a 1:150 weakening of hostile to mouse fluorescein isothiocyanate-conjugated immunoglobulin G immunizer. Three inde-swinging investigations were performed and three arbitrary fields were examined in each slide utilizing an Axio Vert. A1 Carl Zeiss fluorescence magnifying instrument at ×1000 amplification under oil inundation.

Information examination

Each (cell) analyze was performed with three natural repli-cates with every special example in copy. Results were communicated as mean \pm standard mistake (SE) aside from cytotoxicity results that were communicated as mean \pm standard deviation (SD). Contrasts between bunches were assessed utilizing investigation of change (ANOVA) with the exception of cytotoxicity test results that were assessed utilizing unpaired two-followed Student's t-test. For the MN examine, four free measures were performed, and the information were broke down by single direction ANOVA and the gatherings were contrasted and control by Dunnett's test. Contrasts were viewed as critical with a P esteem <0.05.

Results

Molecule characterisation

SEM portrayal

The SEM characterisation uncovered that the TiO₂ powder comprises of particles of various sizes and that it contains marginally to adjusted standard ticles (Figure 1). The characterisation of the essential size of the molecule was performed from a few photos of every molecule. The manufac-turer's data on the NPs was confirmed, estimating a range from 10 to 30 nm (while the producer demonstrated 15–25 nm) and on the MPs (estimating over 100 nm as showed by the manufac-turer). Moreover, the characterisation made by Weir et al. on the E171 can be affirmed, in light of the fact that an extent of

39% NPs and 61% MPs was found, while Weir et al. discovered 36% NPs and 64% MPs (4). To complete, the closeness of the three-dimensional structures of E171, TiO₂ NPs and MPs were affirmed by SEM. Agglomeration and conglomeration can be seen on the various pictures. Agglomerates/totals of tens to several nanometres were shaped with sur-face abnormalities which compare to the single particles.

Characterisation by DLS

Hydrodynamic size and zeta capability of E171 were described utilizing a Malvern Nano ZS DLS instrument. Particles were then dis-persed in medium DMEM + 0.05% BSA, in HBSS cradle and in McCoy + 10% FBS at two distinct fixations: 0.001 and 1 mg/mL (0.143 and 143 µg/cm² individually).

Despite the fact that a few examples have a high polydispersity file, the pres-ence of serum lessens the agglomeration of the particles after 30 min of sonication (40 kHz; Table 1). The stock suspension of 1 mg/mL has the most minimal hydrodynamic size at 316.8 ± 282.4 powerful nm (d.nm) with E171 in McCoy + 10% FBS and the most elevated size at 3085.00 ± 187.82 d.nm with E171 in HBSS. This can likewise be watched for the MPs at a grouping of 1 mg/mL and the NPs at a centralization of 0.001 mg/mL. This shows the significance of serum to improve the scattering and the solidness of the suspension. There is a noteworthy size distinction between the nearness and the nonappearance of serum at a convergence of 1 mg/mL: without included serum (HBSS), the normal hydrodynamic size of the particles is higher than 1000 d.nm for all examples, while with serum it begins at 669.62 ± 17.40 d.nm. All sizes are in the smaller scale go with the exception of in HBSS which has its first size at 5.34 d.nm.

The aftereffects of the 1.10–3 mg/mL demonstrate a few unique sizes relying upon the sort of molecule and suspension. All sizes of MPs and NPs are in the miniaturized scale extend. Shockingly, E171 has the low-est hydrodynamic size in DMEM (316.).

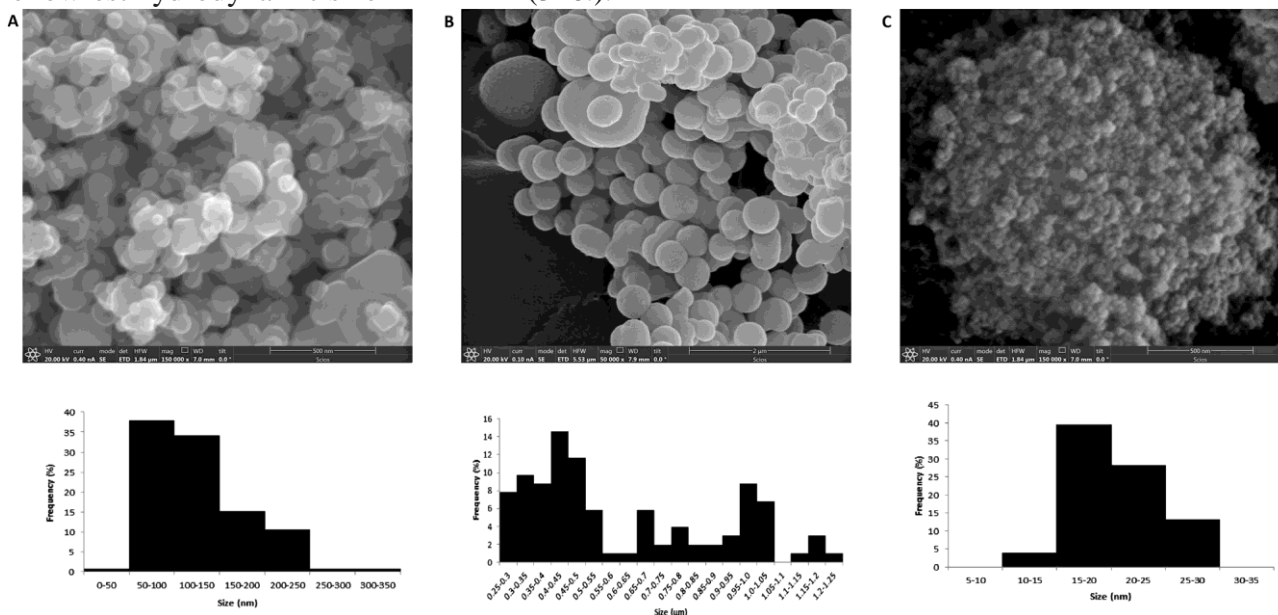


Figure 1. Representative SEM of E171 particles. (A) E171, (B)TiO₂ MPs, (C)TiO₂ NPs. Under each picture histogram of the characterisation of the particle is shown.

concentrations were tested, this difference between the buffer and the medium can be explained by the addition of serum even at low concentrations (0.05%) leads to more colloidal stability which results in a decrease of aggregation and agglomeration of the par- ticles hence to a slightly more stable suspensions. However, the zeta potential values are between −30 mV and +30 mV, which indicate that

the suspensions remain unstable (40,41).

Cytotoxicity of E171, MPs and NPs

E171 reached its cytotoxic concentration at 14.3 $\mu\text{g}/\text{cm}^2$ (0.1 mg/ mL) after 24 h of exposure and the viability of Caco-2 decreased 27%. The exposure to 143 $\mu\text{g}/\text{cm}^2$ induced a decrease of 73% in cell viability. As shown in [supplementary Figure 1](#), available at *Mutagenesis* Online, the cell counter differentiates the alive cells from the dead ones even with this high concentration, interaction of the test with the particles is not responsible of this low cell viability. Exposure to 143 $\mu\text{g}/\text{cm}^2$ of MPs and NPs induced a decrease of 33% and 48.4%, respectively ([Figure 2](#)). Further studies with E171 were performed at non-cytotoxic concentrations of 1.43 and 14.3 $\mu\text{g}/\text{cm}^2$.

HCT116 cells did not show signs of cytotoxicity up to the concentration of 100 $\mu\text{g}/\text{cm}^2$ ([Figure 3](#)).

ROS quantification under cell-free conditions

The capacity of the particles to produce ROS under cell-free conditions was investigated ([Figure 4](#)). Suspensions of E171 particles were prepared in HBSS prior to testing. The particles were also tested in medium with 0.05% BSA, which showed no ROS production (data not shown). This can be attributed to the presence of proteins present in BSA, which form a protein corona that scavenges ROS. E171 had the highest capacity to produce ROS in suspensions with the concentration of 143 $\mu\text{g}/\text{cm}^2$ ([Figure 4](#)) followed by NPs in the presence of H_2O_2 . At a concentration of 14.3 $\mu\text{g}/\text{cm}^2$, NPs induce significant amounts of ROS compared with the control. However, MPs do not generate ROS ([Figure 4](#)). The presence of H_2O_2 does not enhance the formation of ROS by the particles.

Table 1. DLS measurements; size in intensity (d.nm) of the different particles (E171, MPs and NPs) dispersed in DMEM with 0.05% BSA or in HBSS supplemented with Ca^{2+} and Mg^{2+} or Mc Coy +10% FBS and zeta potential results of E171, MPs and NPs with the same conditions as DLS

Dispersant	Sample	Concentration (mg/mL)	Peak (d.nm)	1 Peak (d.nm)	2 Peak (d.nm)	3 Peak (d.nm)	PI	Zeta potential (mV)	
HBSS	E171	1	>1000	-	-	-	0.23 ± 0.03	-4.39 ± 0.12	
		0.01	978.53 ± 59.59 ^a	-	-	-	0.71 ± 0.06	-6.28 ± 1.56 ^a	
		0.001	5.34 ^b	644.40 ^b	>1000 ^b	-	0.76 ± 0.11	-15.03 ± 1.62	
	MP	1	>1000	-	-	-	0.14 ± 0.02	-5.62 ± 0.09	
		0.001	639.43 ± 332.95 ^a	>1000	-	-	0.76 ± 0.06	-6.95 ± 0.62	
	NP	1	>1000	-	-	-	0.15 ± 0.05	-6.08 ± 0.09	
		0.001	>1000 ^a	-	-	-	0.69 ± 0.15	-8.02 ± 0.69	
	DMEM + 0.05% BSA	E171	1	669.62 ± 30.13	-	-	-	0.30 ± 0.02	-12.97 ± 0.29
			0.001	354.48 ± 65.66	1045.13 ± 272.82	>1000	-	0.57 ± 0.03	-12.78 ± 0.52
		MP	1	1385.83 ± 38.85	-	-	-	0.17 ± 0.04	-14.10 ± 0.56
			0.001	1089.10 ± 158.93 ^a	>1000	-	-	0.67 ± 0.09	-13.40 ± 0.44
		NP	1	>1000	-	-	-	0.12 ± 0.03	-13.12 ± 0.44

		0.001	1212.5 332.5 ^a	± -	-	-	0.75 ± -10.66 ±	
	Contr	-	15.34 2.58 ^a	± 165.4 38.5 ^a	± 680.25 10.55 ^a	± >100 ^a	0.10 ± 0.98 0.60 ± -6.18 ±	
Mc Coy + 10% FBS	E171	1	316.8 282.4	± >1000	-	-	0.09 ± 1.35 0.39 ± -12.56 ± 8.3	
		0.01	296.3 367.8	± 226.9 310.3	± 23.9	3.1	0.07 ± -11.9 ± 0.21 ± 0.55	
		0.001	70.78 ± 0.37	-	-	-	0.26 ± -12.56 ± 0.01 0.06	

^aOne or more reads PI > 0.7.

^bOne sample reads P I < 0.7.

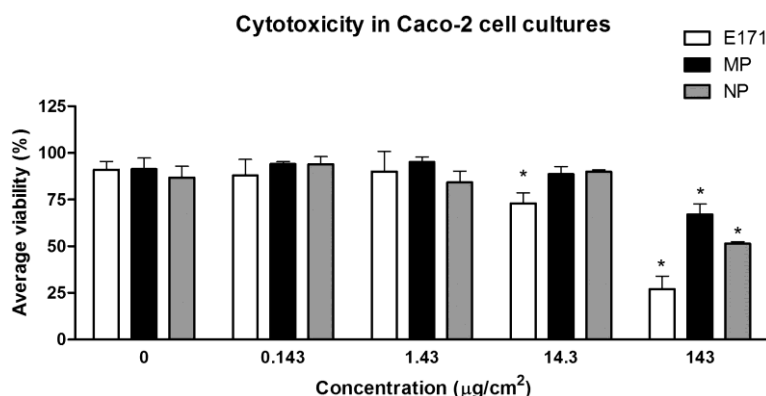


Figure 2. Cytotoxicity in Caco-2 cells after 24 h exposure to E171, MPs and NPs in DMEM plus 0.05% BSA measured by Trypan blue viability test. Statistically significant changes and differences are indicated by an asterisk (* $P < 0.05$, mean \pm SD). Three independent experiments were performed.

ROS evaluation in Caco-2 cells presented to particles

As recently clarified, HBSS cradle was picked as scattering sus-benefits for the estimation of ROS since no ROS arrangement was recognized when particles were scattered in 0.05% BSA medium. Initial, a period course was performed, which indicated that the best introduction time to watch ROS arrangement is 1 h (information not appeared). Figure 5 shows the pinnacle stature determined from the DMPO-OH signal acquired from cell radical development.

Caco-2 cells presented to MPs at a grouping of 1.43 µg/cm² produce noteworthy measures of ROS. For sure, these outcomes were the most steady ones with a lower SD. The ESR machine is extremely delicate, the SD can contrast because of organic contrasts with the nearness of cells. A noteworthy degree of ROS development was additionally decided when cells were presented to MPs at the most reduced non-cytotoxic fixation (1.43 × 10⁻¹ µg/cm²) of MPs co-presented to H₂O₂. Either with or without H₂O₂, no huge ROS development was found after E171 or NPs introduction when contrasted with the control. In a cell environ-ment, just MPs were fit for actuating ROS creation, though E171 and NPs didn't incite ROS.

We theorized that E171 upgrades the genotoxic impacts of AOM in Caco-2 cells through the creation of ROS. Hence, Caco-2 cells were presented at the same time to the genotoxic compound AOM and to E171, MPs and NPs at non-cytotoxic focuses. Co-introduction of AOM didn't prompt critical expanded ROS levels when contrasted with AOM alone. No critical contrast was found between TiO₂ presentation and introduction to AOM of Caco-2 cells (Figure 5).

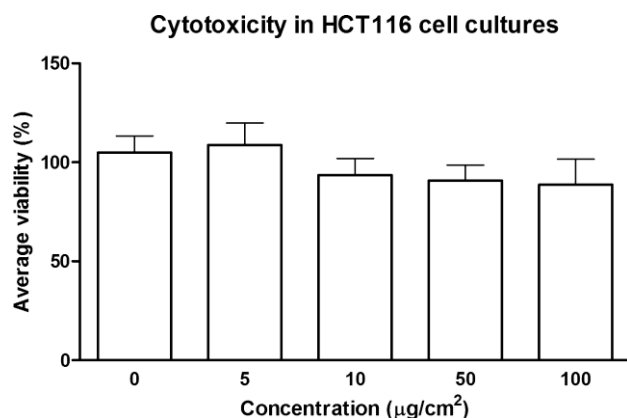


Figure 3. Cytotoxicity in HCT116 cells after 24 h exposure to E171 measured by Trypan blue viability test. There are no statistically significant changes and differences. Three independent experiments were performed.

Single-strand DNA breaks in Caco-2 cell cultures exposed to E171, MP and NPs

The degree of single-strand DNA breaks and antacid labile destinations including abasic locales were surveyed by the comet measure and the middle tail intensity was fundamentally higher after presentation to H Oas contrasted with AOM. Cells were co-uncovered with various particles: E171, NPs or MPs with or without AOM. The outcomes show that E171, MPs and NPs had an ability to instigate single-strand DNA breaks in Caco-2 cells either with or without the nearness of AOM (Figure 6). For the NPs, another non-cytotoxic fixation was tried, no portion reaction on these particles is watched.

E171 initiated chromosome harm in HCT116 cell societies

To examine whether single-strand DNA breaks prompted by E171 presentation could bring about additional chromosome harm, we chose HCT116 as a chromosomally steady cell line to play out a MN measure (42) under non-cytotoxic conditions. In the first place, we uncovered HCT116 cell societies to 5, 10, 50 and 100 µg/cm² of E171 and no decline in cell feasibility was discovered estimated by Trypan blue test (Figure 3). We found an expansion in MN arrangement (Figure 7A) of 1.9-, 2.4- and 3.6-crease of increment in cell societies presented to 5, 10 and 50 µg/cm², separately (Figure 7B). Recurrence of binucleated

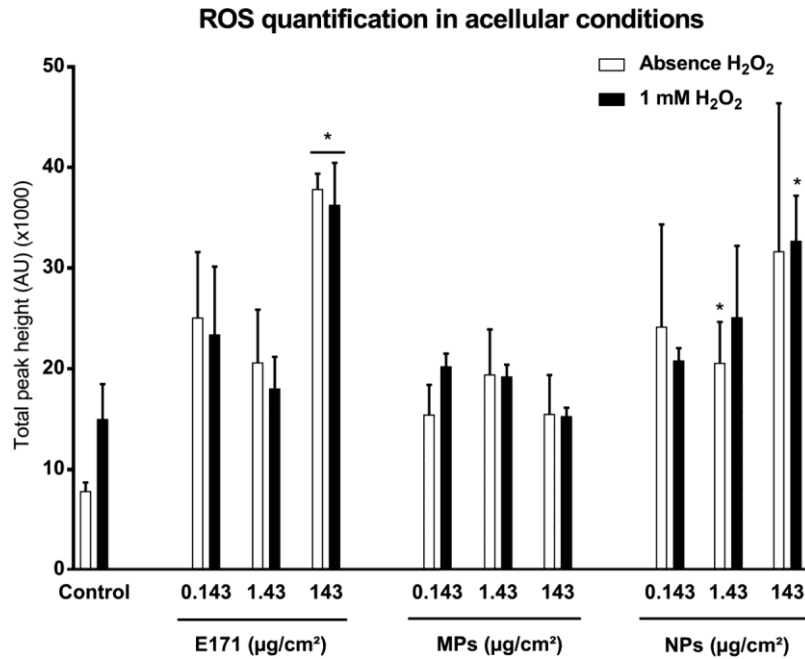


Figure 4. Intensity of cell-free radical formation with various concentrations E171, MPs and NPs in HBSS in the presence (1 mM) or absence of H₂O₂ shown on x-axis. The y-axis represents the average total peak height of obtained ESR spectra calculated per sample. Results include background levels. *P < 0.05: significant difference compared with the control (mean ± SE). No significant difference was found when the presence and absence of H₂O₂ were compared. Three independent experiments were performed.

ROS quantification in Caco-2 exposed cell culture in presence and absence of AOM

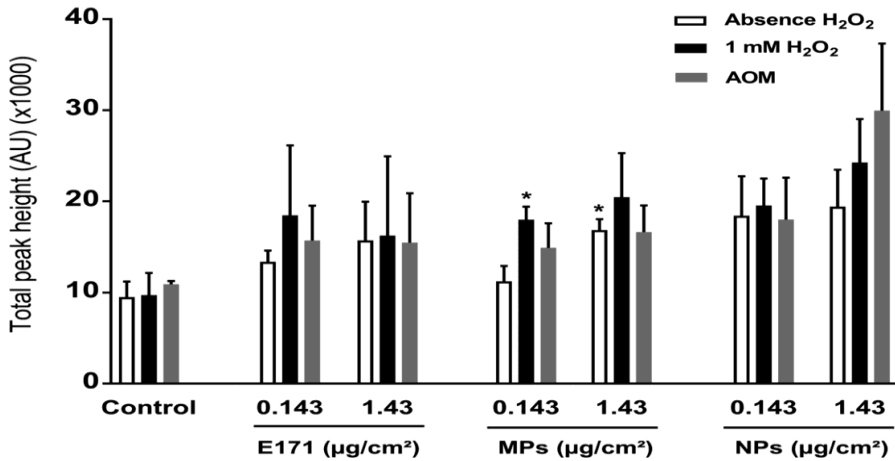


Figure 5. Intensity of cellular radical formation at non-cytotoxic concentrations E171, MPs and NPs in HBSS in cellular (Caco-2) co-exposed to 1 mM of H₂O₂ or 20 µg/mL AOM shown on x-axis. The y-axis represents the average total peak height of obtained ESR spectra calculated per sample. Significant difference compared with the control (*P < 0.05, mean ± SE). Three independent experiments were performed, each of them was performed in duplicate, n = 12.

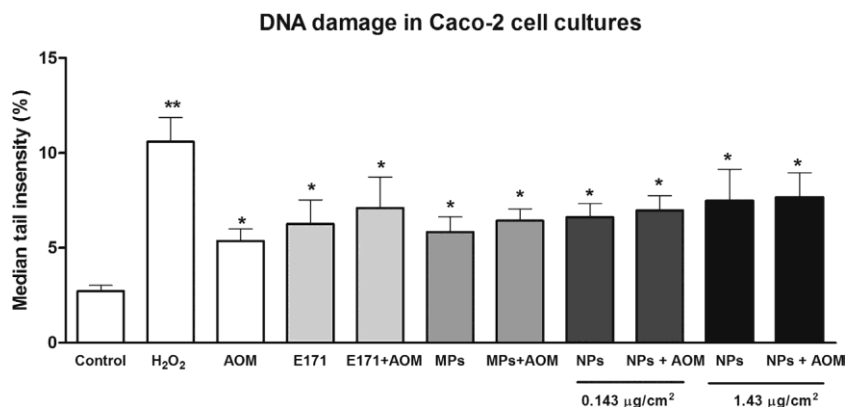


Figure 6. DNA damage in Caco-2 cells after 24h exposure to E171, MPs and NPs. All treatments were at a non-cytotoxic concentration of 0.143 µg/cm² with or without co-exposure of AOM. For the NPs a higher non-cytotoxic concentration was added, 1.43 µg/mL with and without AOM. Thirty minutes exposure of 200 µM H₂O₂ was used as positive control, AOM; 20 µg/mL AOM. DNA damage is represented by median tail intensity shown at y-axis. All conditions are compared with the control (*P < 0.05, **P < 0.001; mean ± SE). The average is from four independent experiments, each of them was performed in duplicate and every sample was on two slides, n = 16.

cells with micronucleus in 1000 binucleated cells after introduction to 5, 10 and 50 µg/cm² of E171 was 1.76, 3.3, 4.1 and 6.6%, regard ively. MN in cells presented to 100 µg/cm² couldn't be surveyed.

E171 communication with the kinetochore

Since DNA harm could be credited to E171 communication during dismantling of atomic envelope for cell division, we explored whether E171 can connect with kinetochores in uncovered HCT116 cell societies. E171 appears to cooperate with the centromere locale of kinetochore posts during mitosis (Figure 8). The association of particles with the shafts of centromeres seems, by all accounts, to be a co-limitation of E171 with α-tubulin, in this manner proposing that E171 particles were appended to DNA of mitotic cells (Figure 8).

Conversation

We found that TiO₂ particles as they are available in the food addi-tive E171 can instigate ROS arrangement and DNA harm in colon-inferred Caco-2 and HCT116 cell lines. These impacts may to some extent clarify prior discoveries of assistance of colon tumor development in a creature model after ingestion of applicable amounts of E171 (28). Impacts were reliant on the size of the particles; to be sure, MPs instigated ROS

development in cell condition, while all particles incited DNA harm. So as to evaluate the association of the parti-cles with the medium and cradle, the particles were described and the zeta potential was resolved utilizing DLS (Table 1). A scattering operator, for example, BSA or FBS is expected to settle and scatter E171, TiO₂ NPs and MPs, as of now appeared for changed nanomaterials including TiO₂ (43,44) and has been applied in bigger orchestrated investigations on nanomaterials genotoxicity (45). We watched less aggre-gation and noticed that E171, NPs or MPs were progressively steady, while their hydrodynamic size was altogether lower in medium with 0.05% BSA or medium with 10% FBS than in HBSS support.

To evaluate the cytotoxicity of the particles, a Trypan blue viabil-ity measure was performed. At first, we applied the MTT and LDH measure (information not appeared), however we discovered obstruction between TiO₂

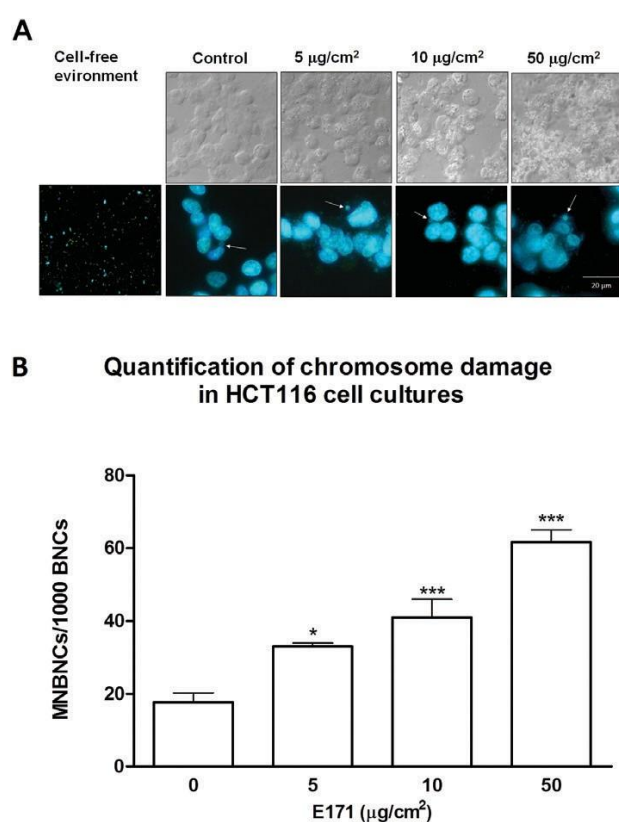


Figure 7. E171 induced chromosome damage in HCT116 cell cultures.

(A) Representative images of HCT116 micronucleated binucleated cells (MNBNCs) after E171 exposure (5, 10, 50 and 100 µg/cm²) for 24 hours. Upper panel shows differential interference contrast in which E171 particles is shown as white agglomerates. Lower panel shows DNA stained by Hoesch dye and MN formation is shown by white arrows. Three independent experiments were performed. (B) Quantification of chromosome damage in HCT116 cell cultures. Number of MNBNCs in 1000 binucleated cells (BNCs) are represented in y-axis. Statistically significant changes and differences are indicated by an asterisk (**P* < 0.05, ***P* < 0.01, ****P* < 0.0001; mean ± SD). Three independent experiments were performed.

also, reasonability measures like LDH, MTT and WST-1. Such obstruction is additionally detailed by others (30,46,47). Consequently, we applied the Trypan blue test. The impedance with the Trypan blue measure was dodged by checking an eye on the screen of the cell counter whether the cells labeled by Trypan blue compare to living Caco-2 cells or not. Moreover, the consequences of the cell counter were compared with the one done at the magnifying lens straightforwardly and these corroborate (strengthening Figure 1, accessible at Mutagenesis Online). The outcomes indicated that E171 is cytotoxic in Caco-2 cells at a lower fixation than the NPs and MPs. Be that as it may, E171 has no poisonous impacts in HCT116 cell societies at fixations utilized in this examination (5, 10, 50 and 100 $\mu\text{g}/\text{cm}^2$) (Figure 2).

As E171 involves 39% NPs and 61% MPs (Figure 1), which affirms past discoveries by Weir et al. (4), we propose that the combination of NPs and MPs is more cytotoxic to Caco-2 cells than NPs or MPs alone. Different examinations (13,48) just focussed on TiO₂ NPs, and fewer contemplations have been performed utilizing TiO₂ food grade. In accordance with our information, fixations up to 0.1 mg/mL TiO₂ NPs (in this investigation it relates to 14.3 $\mu\text{g}/\text{cm}^2$) were likewise seen as non-cytotoxic in human lung epithelial cells (49) with the Trypan blue prohibition tests. Furthermore, in other cell lines, for example, human neural cells and ordinary fibroblasts, MPs and NPs are similarly compelling in instigating cell passing in human neural cells and typical fibroblasts (50). This infers a few impacts are not just because of the size of the particles. Moreover, we propose that molecule aggregation is diverse in Caco-2 and HCT116 cells, in light of the fact that nanoparticle disguise relies upon cell type, as it has been exhibited that disguise of gold nanoparticles estimated in 50 nm is roughly 2-fold higher in macrophages than in human liver disease cells after 24 h of introduction (51).

Likewise, regardless of whether the two sorts of cells are epithelial cultures got from colon, the cytotoxicity of E171 particles can be lower in HCT116 cells (Figure 3), initially, on the grounds that the modular chromosome number at 45 in this cell line gives higher genomic security than Caco-2 cells, which have a stemline modular chromosome number of 96 (<http://www.atcc.org/items/all/HTB-37.aspx#characteristics>). Also, HCT116 cell line has a p16 mutation that prompts expanded expansion with avoidance of cell cycle capture (52,53).

In light of these information, we utilized equivalent non-cytotoxic fixations for each of the three sorts of particles for additional examinations on ROS development in a sans cell condition and in cell societies and for setting up the enlistment of DNA harm in Caco-2 cells. HCT116 cells were chosen for MN estimations since Caco-2 cells like numerous other cell lines are chromosomally instable and subsequently not appropriate for this measure (42).

Various examinations affirm that TiO₂ particles can incite ROS creation (10,54–57). Poisonousness interceded by oxidative worry after presentation to TiO₂ NPs and MPs has been recently portrayed in other gatherings (55,58,59); in any case, MPs demonstrated lower power in ROS age (60), however TiO₂ NPs introduction can cause DNA sores (10,55–57). In our investigation, particles in 0.05% BSA show no ROS development, though without

BSA (HBSS) expanded degrees of ROS were watched both under cell and sans cell conditions (Figures 4 and 5). Along these lines, we reason that BSA scavenges ROS that are shaped on the outside of the particles or may forestall ROS arrangement by hindering the contact between molecule surface and ROS antecedents. In a sans cell condition, E171 and NPs initiate fundamentally higher ROS creation when contrasted with the control (Figure 4). These outcomes are in concurrence with the discoveries of Zijno et al. who have tried TiO₂ NPs with ESR spectroscopy and furthermore watched ROS creation in a sans cell condition (14). As opposed to E171 and NPs, MPs don't incite any ROS creation when they are scattered in cushion (Figure 4).

In a cell situation, the limit of E171 and NPs to star duce ROS was unequivocally diminished while just MPs were fit for creating ROS (Figure 5). We propose that MPs by means of ROS production would actuate a genius fiery reaction. This was at that point saw in a co-culture of intestinal cells and macrophages presented to TiO₂ MPs in which the group estimated an upregulation of star fiery caspases and cytokines, for example, caspase-1 and IL-1 β and IL-18 (61). Besides, another gathering watched a Th1-interceded provocative reaction in the little gut in mice.(62)

We as of late found that E171 in vivo presentation improved the quantity of tumors in the colon of mice presented to AOM/DSS (28). The joined presentation to AOM/DSS is regularly utilized for the concoction acceptance of colonic tumors in creature tests where AOM goes about as a DNA alkylation reagent starting the cancer-causing process (63). So as to reveal insight into the instruments behind these in vivo outcomes, we co-uncovered Caco-2 cells to AOM and TiO₂ standard ticles (E171, NPs and MPs) and performed ESR spectrometry and a comet examine to identify single-strand DNA breaks and soluble base labile locales. To test the impact of AOM on ROS arrangement, Caco-2 cells were co-presented to AOM and E171, NPs or MPs. ROS levels were not altogether extraordinary between cells that were just presented to the particles and cells that were co-presented to AOM (Figure 5). This shows the expanded tumor development in mice probably won't be ascribed to ROS. Further in vitro and in vivo examinations, for example, full genome articulation investigation, should be performed to have the option to con-clude about the instruments behind the possible cancer-causing impact of E171.

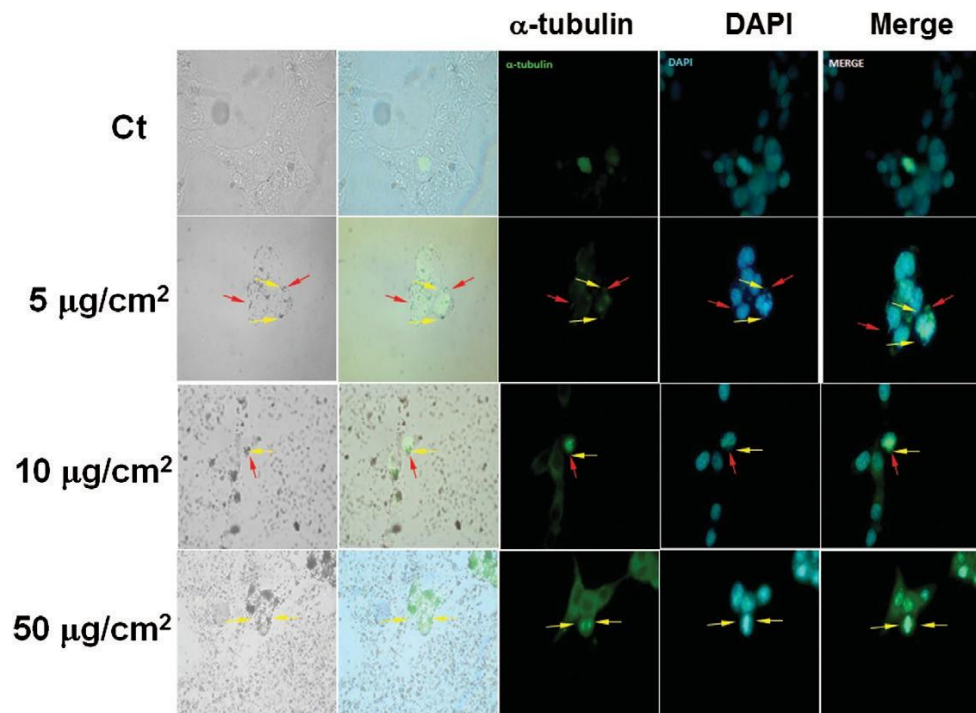


Figure 8. Identification of E171 interaction with kinetochores. HCT117 cell cultures were exposed to E171 particles (5, 10, 50 and 100 $\mu\text{g}/\text{cm}^2$). A positive E171 interaction with mitotic kinetochore poles is shown by yellow arrows. E171 particles co-localized with mitotic genome and α -tubulin is showed by red arrows. Untreated cell had no presence of particles.

The nonattendance of ROS acceptance by E171 and NPs in our examination might be clarified by the way that after disguise, particles respond promptly with cell structures that square ROS creation. Without a doubt, the NPs segment would enter the cells as appeared by Shukla et al. where they show that the NPs of TiO₂ can without much of a stretch enter the cell and even arrive at the core of human epidermal cells (32). In the wake of entering the phone, the radicals created by the particles could then diminish the phone glutathione (GSH) content as appeared by Shlukla et al. where they uncovered human epidermal cells to TiO₂ NPs and watched a noteworthy decrease of cell GSH content from 8 µg/mL(32). This would help to restore the redox balance. However the capacity of E171 and NPs to associate with different biomolecules could prompt cell changes, including protein, RNA and DNA adjustments.

The consequences of the comet test indicated that E171 and TiO₂ NPs and MPs are genotoxic by inciting single-strand DNA breaks and no portion reaction was found for the NPs, with the genotoxicity being the equivalent (Figure 6). Furthermore, E171 causes chromosome harm in the HCT116 cell line estimated by the micronucleus examine (Figure 7). As micronucleus is a part of DNA, it is relied upon to distinguish it by a blue recoloring by Hoechst color. At that point, micronucleus can be seen as roundabout shapes with smooth edges. The basal degrees of micronucleus recurrence in our outcomes concur with past writing, which are evaluated somewhere in the range of 2.5% and 3.2% (64,65).

The outcomes from two distinctive cell lines demonstrate the in vitro gen-otoxicity of E171. DNA harm might be the result of E171 interfacing with microtubules, as appear to happen in HCT116 cells, which could occur during the atomic envelope dismantling that goes before mitosis. The collaboration among E171 and microtubules from the kinetochores could prompt chromosome missegregation and the arrangement of MN (66) (Figure 8). Moreover, genotoxicity is known to assume a significant job in the commencement condition of carcinobeginning since it can prompt changes in the hereditary material bringing about modifications on cell flagging pathways identified with cell multiplication and apoptosis (62). We along these lines estimate that E171 genotoxicity in colon cells could be taking an interest in cancer-causing procedures, for example, upgrading tumor arrangement in an azoxymethane-actuated colorectal malignant growth model by intragastric E171 particles organization (28).

The colon is the significant site for supplement take-up yet conceivably additionally for perilous aggravates that can be available in the food. The E171 particles, known as food TiO₂ added substance, is available in a wide range of sorts of food. It is hard to correspond between in vitro and in vivo fixations in the gut without making a number of suppositions. By the by, we made an estimation of the concentration of TiO₂ in the colon accepting the normal introduction of a grown-up to be 1 mg/kg body weight/day (4), a normal load of 70 kg and an amount of dung discharged every day somewhere in the range of 100 and 250 g/day. On the off chance that we make a traditionalist gauge, the grown-up of 70 kg would ingest 70 mg of TiO₂ every day, this individual would create 250 g of dung that would make a grouping of TiO₂ in the defecation of 0.28 mg of TiO₂/g of excrement. Dung contain 75% of water, so on the off chance that we consider that the thickness of excrement is equivalent to water, the grouping of TiO₂ would be 0.28 mg/mL of defecation. On the off chance that we accept that just 1% of these is organically accessible for presentation, 0.0028 mg/mL of TiO₂ is conceivably arriving at the colon cells. The non-cytotoxic convergences of TiO₂ utilized during the in vitro tries are 0.01 mg/mL and 0.001 mg/mL. Along these lines, the concentrations are in a similar significant degree as the evaluated convergence of TiO₂ in the colon. Apparently, this is the first occasion when that the genotoxicity of E171 and distinctive size portions were appeared in colon-inferred cell societies. The discoveries of the present in vitro examination exhibit that TiO₂ as food additives coded as E171, even at the least focus tried, have DNA harming potential in human colonic cells and that the MPs in E171 may be the most significant for ROS arrangement as appeared within the sight of Caco-2 cells. The ability to create ROS and to incite DNA harm raises worries about the protected utilization of E171 in various food items.

References

1. Lomer, M. C., Thompson, R. P., Commisso, J., Keen, C. L. and Powell, J. J. (2000) Determination of titanium dioxide in foods using inductively coupled plasma optical emission spectrometry. *Analyst*, 125, 2339–2343.
2. Peters, R. J., van Bommel, G., Herrera-Rivera, Z., *et al.* (2014) Characterization of titanium dioxide nanoparticles in food products: analytical methods to define nanoparticles. *J. Agric. Food Chem.*, 62, 6285–6293.
3. Shi, H., Magaye, R., Castranova, V. and Zhao, J. (2013) Titanium dioxide nanoparticles: a review of current toxicological data. *Part. Fibre Toxicol.*, 10, 15.
4. Weir, A., Westerhoff, P., Fabricius, L., Hristovski, K. and von Goetz, N. (2012) Titanium dioxide nanoparticles in food and personal care products. *Environ. Sci. Technol.*, 46, 2242–2250.
5. EU. (2012) Regulation No 231-2012 on food additives. *OJL*, 83, 1–295.
6. USFDA. (2016) *US Food and Drug Administration regulation on titanium dioxide. Code of Federal Regulations, Title 21, Section 73.575.* US Food and Drug Administration, Silver Springs, MD.
7. Bhattacharya, K., Davoren, M., Boertz, J., Schins, R.P., Hoffmann, E. and Dopp, E. (2009) Titanium dioxide nanoparticles induce oxidative stress and DNA-adduct formation but not DNA-breakage in human lung cells. *Part. Fibre Toxicol.*, 6, 17.
8. Falck, G. C., Lindberg, H. K., Suhonen, S., Vippola, M., Vanhala, E., Catalán, J., Savolainen, K. and Norppa, H. (2009) Genotoxic effects of nano-sized and fine TiO₂.

- Hum. Exp. Toxicol.*, 28, 339–352.
9. Kang, S. J., Kim, B. M., Lee, Y. J. and Chung, H. W. (2008) Titanium dioxide nanoparticles trigger p53-mediated damage response in peripheral blood lymphocytes. *Environ. Mol. Mutagen.*, 49, 399–405.
 10. Wang, J. J., Sanderson, B. J., and Wang, H. (2007) Cytotoxicity and genotoxicity of ultrafine TiO₂ particles in cultured human lymphoblastoid cells. *Mut. Res.*, 628, 99–106.
 11. Armand, L., Tarantini, A., Beal, D., *et al.* (2016) Long-term exposure of A549 cells to titanium dioxide nanoparticles induces DNA damage and sensitizes cells towards genotoxic agents. *Nanotoxicology*, 10, 1–11.
 12. IARC. (2010) *IARC Monographs on the Evaluation of Carcinogenic Risks to Humans: Carbon Black, Titanium dioxide and Talc*, Vol. 93. International Agency for Research on Cancer, Lyon, France.
 13. Gerloff, K., Albrecht, C., Boots, A. W., Forster, I., and Schins, R. P. F. (2009) Cytotoxicity and oxidative DNA damage by nanoparticles in human intestinal Caco-2 cells. *Nanotoxicology*, 3, 355–364.
 14. Zijno, A., De Angelis, I., De Berardis, B., *et al.* (2015) Different mechanisms are involved in oxidative DNA damage and genotoxicity induction by ZnO and TiO nanoparticles in human colon carcinoma cells. *Toxicol. In Vitro*, 29, 1503–1512.
 15. Dorier, M., Brun, E., Veronesi, G., *et al.* (2015) Impact of anatase and rutile titanium dioxide nanoparticles on uptake carriers and efflux pumps in Caco-2 gut epithelial cells. *Nanoscale*, 7, 7352–7360.
 16. Song, Z. M., Chen, N., Liu, J. H., *et al.* (2015) Biological effect of food additive titanium dioxide nanoparticles on intestine: an in vitro study. *J. Appl. Toxicol.*, 35, 1169–1178.
 17. Tarantini, A., Lanceleur, R., Mourot, A., Lavault, M. T., Casterou, G., Jarry, G., Hogeveen, K. and Fessard, V. (2015) Toxicity, genotoxicity and proinflammatory effects of amorphous nanosilica in the human intestinal Caco-2 cell line. *Toxicol. In Vitro*, 29, 398–407.
 18. Robichaud, C. O., Uyar, A. E., Darby, M. R., Zucker, L. G. and Wiesner, M. R. (2009) Estimates of upper bounds and trends in nano-TiO₂ production as a basis for exposure assessment. *Environ. Sci. Technol.*, 43, 4227–4233.
 19. Pan, Y., Leifert, A., Ruau, D., Neuss, S., Bornemann, J., Schmid, G., Brandau, W., Simon, U. and Jahnke-Dechent, W. (2009) Gold nanoparticles of diameter 1.4 nm trigger necrosis by oxidative stress and mitochondrial damage. *Small*, 5, 2067–2076.
 20. Schaeublin, N. M., Braydich-Stolle, L. K., Schrand, A. M., Miller, J. M., Hutchison, J., Schlager, J. J. and Hussain, S. M. (2011) Surface charge of gold nanoparticles mediates mechanism of toxicity. *Nanoscale*, 3, 410–420.
 21. Niska, K., Pyszka, K., Tukaj, C., Wozniak, M., Radomski, M. W. and Inkielewicz-Stepniak, I. (2015) Titanium dioxide nanoparticles enhance production of superoxide anion and alter the antioxidant system in human osteoblast cells. *Int. J. Nanomed.*, 10,

- 1095–1107.
22. Cooke, M. S., Evans, M. D., Dizdaroglu, M. and Lunec, J. (2003) Oxidative DNA damage: mechanisms, mutation, and disease. *FASEB J.*, 17, 1195–1214.
 23. Inoue, S. and Kawanishi, S. (1987) Hydroxyl radical production and human DNA damage induced by ferric nitrilotriacetate and hydrogen peroxide. *Cancer Res.*, 47, 6522–6527.
 24. Jackson, J. H., Schraufstatter, I. U., Hyslop, P. A., Vosbeck, K., Sauerheber, R., Weitzman, S. A. and Cochrane, C. G. (1987) Role of oxidants in DNA damage. Hydroxyl radical mediates the synergistic DNA damaging effects of asbestos and cigarette smoke. *J. Clin. Invest.*, 80, 1090–1095.
 25. Powell, J. J., Ainley, C. C., Harvey, R. S., Mason, I. M., Kendall, M. D., Sankey, E. A., Dhillon, A. P. and Thompson, R. P. (1996) Characterisation of inorganic microparticles in pigment cells of human gut associated lymphoid tissue. *Gut*, 38, 390–395.
 26. Lomer, M. C., Thompson, R. P. and Powell, J. J. (2002) Fine and ultrafine particles of the diet: influence on the mucosal immune response and association with Crohn's disease. *Proc. Nutr. Soc.*, 61, 123–130.
 27. Grissa, I., Elghoul, J., Ezzi, L., *et al.* (2015) Anemia and genotoxicity induced by subchronic intragastric treatment of rats with titanium dioxide nanoparticles. *Mutat. Res. Genet. Toxicol. Environ. Mutagen.*, 794, 25–31.
 28. Urrutia-Ortega, I. M., Garduno-Balderas, L. G., Delgado-Buenrostro, N. L., *et al.* (2016) Food-grade titanium dioxide exposure exacerbates tumor formation in colitis associated cancer model. *Food Chem. Toxicol.*, 93, 20–31.
 29. Hawkins, C. L. and Davies, M. J. (2014) Detection and characterisation of radicals in biological materials using EPR methodology. *Biochim. Biophys. Acta*, 1840, 708–721.
 30. Kroll, A., Pillukat, M. H., Hahn, D. and Schnekenburger, J. (2012) Interference of engineered nanoparticles with in vitro toxicity assays. *Arch. Toxicol.*, 86, 1123–1136.
 31. Jugan, M. L., Barillet, S., Simon-Deckers, A., Herlin-Boime, N., Sauvaigo, S., Douki, T. and Carriere, M. (2012) Titanium dioxide nanoparticles exhibit genotoxicity and impair DNA repair activity in A549 cells. *Nanotoxicology*, 6, 501–513.
 32. Shukla, R. K., Sharma, V., Pandey, A. K., Singh, S., Sultana, S. and Dhawan, A. (2011) ROS-mediated genotoxicity induced by titanium dioxide nanoparticles in human epidermal cells. *Toxicol. In Vitro*, 25, 231–241.
 33. Gonzalez, L., Sanderson, B. J. and Kirsch-Volders, M. (2011) Adaptations of the in vitro MN assay for the genotoxicity assessment of nanomaterials. *Mutagenesis*, 26, 185–191.
 34. Masramon, L., Vendrell, E., Tarafa, G., Capellà, G., Miró, R., Ribas, M. and Peinado, M. A. (2006) Genetic instability and divergence of clonal populations in colon cancer cells in vitro. *J. Cell Sci.*, 119, 1477–1482.
 35. Nymark, P., Jensen, K. A., *et al.* (2014) Free radical scavenging and formation by multi-walled carbon nanotubes in cell free conditions and in human bronchial epithelial cells.

- Part. Fibre Toxicol.*, 11, 4.
36. Briedé, J. J., van Delft, J. M., de Kok, T. M., van Herwijnen, M. H., Maas, L. M., Gottschalk, R. W. and Kleinjans, J. C. (2010) Global gene expression analysis reveals differences in cellular responses to hydroxyl- and superoxide anion radical-induced oxidative stress in caco-2 cells. *Toxicol. Sci.*, 114, 193–203.
 37. Hebels, D. G., Briedé, J. J., Khampang, R., Kleinjans, J. C. and de Kok, T. M. (2010) Radical mechanisms in nitrosamine- and nitrosamide-induced whole-genome gene expression modulations in Caco-2 cells. *Toxicol. Sci.*, 116, 194–205.
 38. Hebels, D. G., Sveje, K. M., de Kok, M. C., *et al.* (2011) N-nitroso compound exposure-associated transcriptomic profiles are indicative of an increased risk for colorectal cancer. *Cancer Lett.*, 309, 1–10.
 39. Fenech, M. (2000) The in vitro micronucleus technique. *Mut. Res.*, 455, 81–95.
 40. Ismail, M. F., Elmeshad, A. N. and Salem, N. A. (2013) Potential therapeutic effect of nanobased formulation of rivastigmine on rat model of Alzheimer's disease. *Int. J. Nanomed.*, 8, 393–406.
 41. Lin, P. C., Lin, S., Wang, P. C. and Sridhar, R. (2014) Techniques for physico-chemical characterization of nanomaterials. *Biotechnol. Adv.*, 32, 711–726.
 42. Thompson, S. L. and Compton, D. A. (2008) Examining the link between chromosomal instability and aneuploidy in human cells. *J. Cell Biol.*, 180, 665–672.
 43. Bihari, P., Vippola, M., Schultes, S., *et al.* (2008) Optimized dispersion of nanoparticles for biological in vitro and in vivo studies. *Part. Fibre Toxicol.*, 5, 14.
 44. Vippola, M., Falck, G. C., Lindberg, H. K., Suhonen, S., Vanhala, E., Norppa, H., Savolainen, K., Tossavainen, A. and Tuomi, T. (2009) Preparation of nanoparticle dispersions for in-vitro toxicity testing. *Hum. Exp. Toxicol.*, 28, 377–385.
 45. Jensen, K. A., Kembouche, Y., Christiansen, E., Jacobsen, N. R., Wallin, H., Guiot, C., Spalla, O. and Witschger, O. (2011) Final protocol for producing suitable manufactured nanomaterial exposure media. *NANOGENO-TOX deliverable report n°3*.
 46. Guadagnini, R., Halamoda Kenzaoui, B., Walker, L., *et al.* (2015) Toxicity screenings of nanomaterials: challenges due to interference with assay processes and components of classic in vitro tests. *Nanotoxicology*, 9, 13–24.
 47. Holder, A. L., Goth-Goldstein, R., Lucas, D. and Koshland, C. P. (2012) Particle-induced artifacts in the MTT and LDH viability assays. *Chem. Res. Toxicol.*, 25, 1885–1892.
 48. Gerloff, K., Fenoglio, I., Carella, E., Kolling, J., Albrecht, C., Boots, A. W., Förster, I. and Schins, R. P. (2012) Distinctive toxicity of TiO₂ rutile/anatase mixed phase nanoparticles on Caco-2 cells. *Chem. Res. Toxicol.*, 25, 646–655.
 49. Prasad, R. Y., Wallace, K., Daniel, K. M., *et al.* (2013) Effect of treatment media on the agglomeration of titanium dioxide nanoparticles: impact on genotoxicity, cellular interaction, and cell cycle. *ACS Nano*, 7, 1929–1942. Lai, J. C., Lai, M. B., Jandhyam, S., Dukhande, V. V., Bhushan, A., Daniels, C. K. and Leung, S. W. (2008) Exposure to titanium dioxide and other metallic oxide nanoparticles induces cytotoxicity on human neural cells and fibroblasts. *Int. J.*

Nanomed., 3, 533–545.

51. Cheng, X., Tian, X., Wu, A., *et al.* (2015) Protein corona influences cellular uptake of gold nanoparticles by phagocytic and nonphagocytic cells in a size-dependent manner. *ACS Appl. Mater. Interfaces*, 7, 20568–20575.
52. Guan, R. J., Fu, Y., Holt, P. R. and Pardee, A. B. (1999) Association of K-ras mutations with p16 methylation in human colon cancer. *Gastro- enterology*, 116, 1063–1071.
53. Hara, E., Smith, R., Parry, D., Tahara, H., Stone, S. and Peters, G. (1996) Regulation of p16CDKN2 expression and its implications for cell immor- talization and senescence. *Mol. Cell. Biol.*, 16, 859–867.
54. Iavicoli, I., Leso, V. and Bergamaschi, A. (2012) Toxicological effects of titanium dioxide nanoparticles: a review of in vivo studies. *J. Nanomater*, 2012, Article ID 96481.
55. Gurr, J. R., Wang, A. S., Chen, C. H. and Jan, K. Y. (2005) Ultrafine titanium dioxide particles in the absence of photoactivation can induce oxidative damage to human bronchial epithelial cells. *Toxicology*, 213, 66–73.
56. Dunford, R., Salinaro, A., Cai, L., Serpone, N., Horikoshi, S., Hidaka, H. and Knowland, J. (1997) Chemical oxidation and DNA damage catalysed by inorganic sunscreen ingredients. *FEBS Lett.*, 418, 87–90.
57. Rahman, Q., Lohani, M., Dopp, E., Pemsel, H., Jonas, L., Weiss, D. G. and Schiffmann, D. (2002) Evidence that ultrafine titanium dioxide induces micronuclei and apoptosis in Syrian hamster embryo fibroblasts. *Environ. Health Perspect.*, 110, 797–800.
58. Ramires, P. A., Romito, A., Cosentino, F. and Milella, E. (2001) The influ- ence of titania/hydroxyapatite composite coatings on in vitro osteoblasts behaviour. *Biomaterials*, 22, 1467–1474.
59. Hussain, S. M., Hess, K. L., Gearhart, J. M., Geiss, K. T. and Schlager, J. J. (2005) In vitro toxicity of nanoparticles in BRL 3A rat liver cells. *Toxicol. In Vitro*, 19, 975–983.
60. Kang, J. L., Moon, C., Lee, H. S., Lee, H. W., Park, E. M., Kim, H. S. and Castranova, V. (2008) Comparison of the biological activity between ultrafine and fine titanium dioxide particles in RAW 264.7 cells associ- ated with oxidative stress. *J. Toxicol. Environ. Health A*, 71, 478–485.
61. Becker, H. M., Bertschinger, M. M. and Rogler, G. (2012) Micropar- ticles and their impact on intestinal immunity. *Dig. Dis.*, 30(Suppl 3), 47–54.
62. Nogueira, C. M., de Azevedo, W. M., Dagli, M. L., *et al.* (2012) Titanium dioxide induced inflammation in the small intestine. *World J. Gastroen- terol.*, 18, 4729–4735.
63. Tanaka, T., Kohno, H., Suzuki, R., Yamada, Y., Sugie, S. and Mori, H. (2003) A novel inflammation-related mouse colon carcinogenesis model induced by azoxymethane and dextran sodium sulfate. *Cancer Sci.*, 94, 965–973.
64. Camps, J., Ponsa, I., Ribas, M., Prat, E., Egozcue, J., Peinado, M. A. and Miró, R. (2005) Comprehensive measurement of chromosomal instabil- ity in cancer cells: combination of fluorescence in situ hybridization and cytokinesis-block micronucleus assay. *FASEB J.*, 19, 828–830.

65. Bakhoun, S. F., Kabeche, L., Wood, M. D., *et al.* (2015) Numerical chromosomal instability mediates susceptibility to radiation treatment. *Nat. Commun.*, 6, 5990.
66. Huang, S., Chueh, P. J., Lin, Y. W., Shih, T. S. and Chuang, S. M. (2009) Disturbed mitotic progression and genome segregation are involved in cell transformation mediated by nano-TiO₂ long-term exposure. *Toxicol. Appl. Pharmacol.*, 241, 182–194.

This work is partly submitted at 19th international conference on Global Toxicology and Risk Assessment in Madrid Spain during November 05-06-2020.

Carolina Rodríguez-Ibarra
GROW Institute of Oncology and Developmental Biology, Mexico
Email id: caro.roib@hotmail.com

[19th international conference on Global Toxicology and Risk Assessment](#)

November 05-06-2020

Volume 9 . Issue 1